

# Architecture Study for a Fuel Depot Supplied from Lunar Assets

Thomas M. Perrin<sup>1</sup>

*Aerodyne Industries, LLC (Jacobs ESSSA Group), Cape Canaveral, FL, 32920*

*and*

James G. Casler<sup>2</sup>

*University of North Dakota, Grand Forks, ND, 58202*

This architecture study sought to determine the optimum architecture for a fuel depot supplied from lunar assets. Four factors – the location of propellant processing (on the Moon or on the depot), the depot location (on the Moon, L1, GEO, or LEO), the propellant transfer location (L1, GEO, or LEO), and the propellant transfer method (bulk fuel or canister exchange) were combined to identify 18 candidate architectures. Two design reference missions (DRMs) – a commercial satellite servicing mission and a Government cargo mission to Mars – created demand for propellants, while a propellant delivery DRM examined supply issues. The study concluded Earth-Moon L1 is the best location for an orbiting depot. For all architectures, propellant boiloff was less than anticipated, and was far overshadowed by delta-v requirements and resulting fuel consumption. Bulk transfer is the most flexible for both the supplier and customer. However, since canister exchange bypasses the transfer of bulk cryogenics and necessary chilldown losses, canister exchange shows promise and merits further investigation. Overall, this work indicates propellant consumption and loss is an essential factor in assessing fuel depot architectures.

## Nomenclature

### A. Calculating outside temperature of the spacecraft

- T = outside temperature of the spacecraft (K)
- $\sigma$  = Boltzmann's constant =  $5.67051 \times 10^{-8} \text{ W/m}^2 \text{ K}^{-4}$
- $\alpha$  = absorptivity
- $\varepsilon$  = emissivity
- S = solar flux ( $1,367 \text{ W/m}^2$ )
- RH = Earth reflected heating
- E = Earth infrared
- $A_p$  = projected area of the propellant tank
- A = total surface area of the propellant tank

### B. Modified Lockheed Model

- Q = heat transfer rate in  $\text{W/m}^2$
- $\varepsilon$  = emissivity of the inner layers of MLI
- $T_h$  = temperature on outside tank surface (K)
- $T_c$  = propellant temperature
- T =  $(T_h + T_c)/2$
- $N^*$  = number of layers/cm of MLI
- $N_s$  = number of layers of MLI
- P = pressure between the layers of MLI (Torr)

---

<sup>1</sup> Sr.Ground Operations Systems Engineer, EO40/Operations Engineering, NASA/Marshall Space Flight Center, AIAA Member

<sup>2</sup> Department Chair, Space Studies Department, 4149 University Ave Stop 9008, AIAA Associate Fellow.

## I. Introduction

A POLLO-era mission design was based on taking everything needed for a mission from the Earth. This was an obvious choice. One reason behind this choice was the challenge by President Kennedy to land on and return from the Moon by the end of the decade. Another reason behind the choice had to do with the limited knowledge of the Moon and its resources. When traveling such a great distance from Earth into the unknown, it only made sense to take everything needed.

However, Earth's deep gravity well makes this paradigm expensive. It has been estimated the space shuttle cost \$18,413/kg to place an object in low earth orbit (LEO).<sup>1</sup> Having to take all the fuel needed for a mission limits the size of the payload that can be taken. It would be far more cost effective to refuel vehicles in space.

The existence of lunar ice was first predicted in 1961 by Watson, Murray, and Brown. They showed that water is actually one of the most stable of the lunar volatiles, and predicted that over the life of the Moon, water could have migrated to the cold traps at the lunar poles.<sup>2</sup> The idea lay dormant until 1979 when Arnold verified the stability of the lunar cold traps and the trapping mechanism and further advocated a lunar mission to search for ice deposits at the lunar poles.<sup>3</sup>

In 1998, NASA launched the Lunar Prospector probe into lunar orbit. Included on board the probe was an instrument called a neutron spectrometer. The experiment searched for and confirmed the presence of hydrogen at the lunar poles which indicated the presence of ice.<sup>4</sup>

In 2009, NASA launched the Lunar Reconnaissance Orbiter (LRO) and Lunar Crater Observing and Sensing Satellite (LCROSS) missions. An Atlas V Centaur upper stage rocket was deliberately impacted into the Cabeus crater on October 9th, and the LCROSS spacecraft flew through the debris kicked up by the rocket. From the data gathered, NASA was able to confirm the presence of water ice. The size of the ice deposits has since been estimated to be as large as 600 million cubic meters.<sup>5</sup>

The confirmation of substantial deposits of water at the lunar poles suggests the Moon could provide liquid oxygen and hydrogen to an orbiting fuel depot. Such a plan represents an In-Situ Resource Utilization (ISRU) - based exploration paradigm – launch from the Earth using terrestrial resources, then use in-situ resources to refuel for the trip home or to maneuver to a more distant destination. A fuel depot would also enable/require the use of vehicles tailored to specific applications – Earth-to-orbit vehicles, Moon-to-orbit vehicles, and dedicated in-space vehicles.

Consideration of an architecture for a fuel depot supplied from lunar resources gives rise to a great many questions. Where, for example, should such a depot be located? How many depots should there be? Should water harvested on the Moon be processed into liquid oxygen and liquid hydrogen on the Moon, or should it be shipped to the depot and processed on the depot itself? And how will the transfer of fuel be accomplished? Would it be better to ship in bulk and wrestle with the transfer of cryogenics in microgravity, or would it be better to ship using standardized canisters, and refuel a customer spaceship simply by exchanging empty canisters for full ones? Regardless of the choices made, there will be a cost to both the supplier and the customer. Both parties will consume propellant in carrying out their respective missions, and both parties will lose propellants due to boiloff. So the research question becomes: What architecture would be the most efficient in terms of propellant consumption and loss? More precisely, what architecture would satisfy customer requirements for the least amount of liquid oxygen (LO<sub>2</sub>) and liquid hydrogen (LH<sub>2</sub>) consumed in flight or lost to boiloff?

## II. Methodology

### A. General Intent

The general intent of this study effort is to create candidate architectures for a fuel depot supported from lunar assets, and to evaluate those architectures on the basis of the mass of propellant consumed and the mass of propellant lost due to boiloff. The discussion here provides an overview of the methodology. Discussions of specific tasks (calculating fuel consumption or boiloff, etc.) are provided in subsequent sections.

### B. Step by Step

Ground rules, assumptions, and constraints are necessary to bound the problem being attempted. Figure 1 provides a list of ground rules, assumptions, and constraints used to simplify the problem without assuming it away.

Candidate architectures are defined by several attributes, including the number of depots proposed, the location of the depot(s), the location where electrolysis will be performed, and the methods of fuel transfer. The candidate architectures are then depicted as a network diagram in Fig. 2. Each candidate architecture is unique, and the choices

made in developing the architecture can be depicted as a separate path in the diagram. The diagram is an excellent method of depicting the candidate architectures, and visualizing relationships.

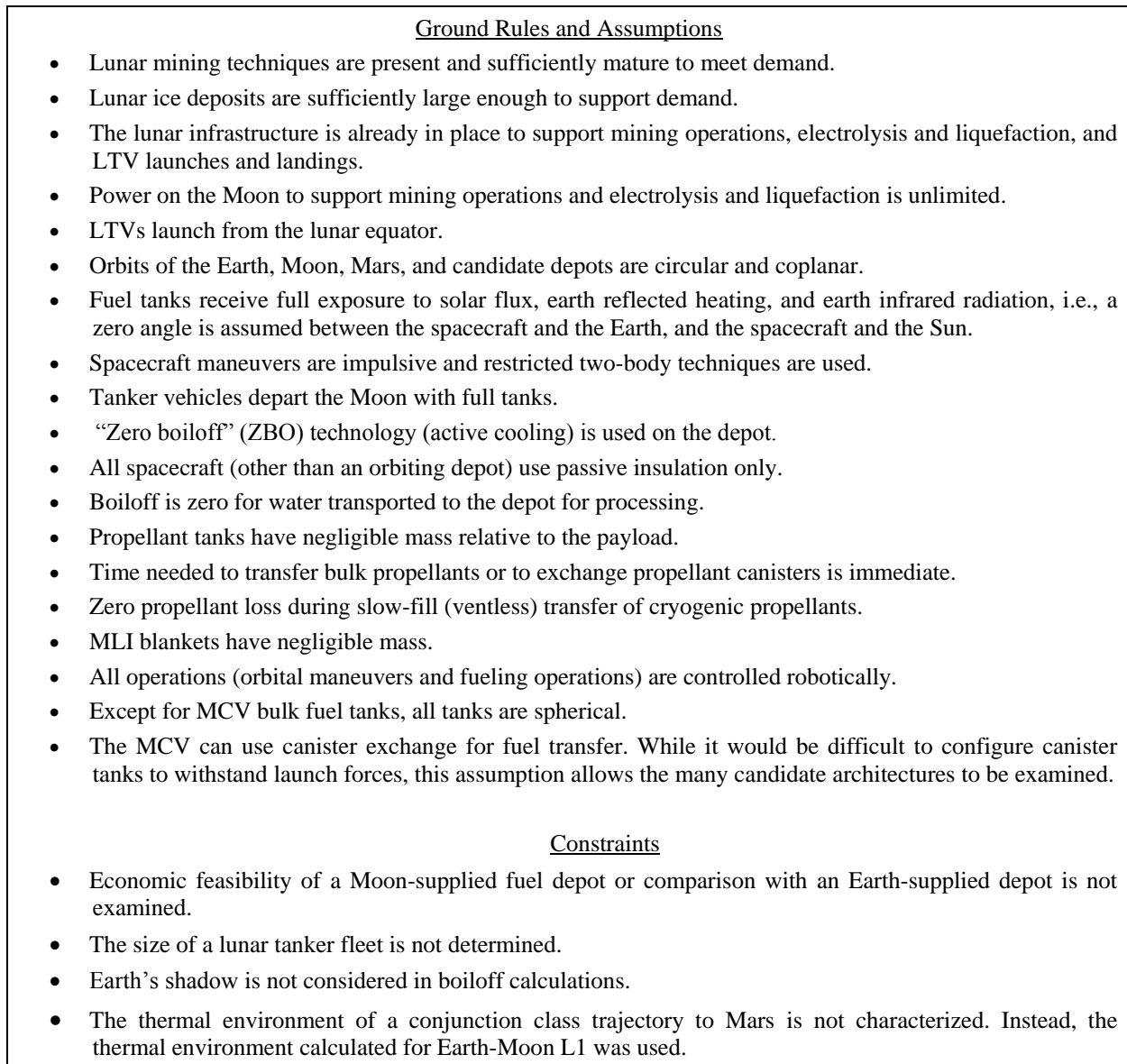


**Figure 1. Ground Rules, Assumptions, and Constraints**

The next step in the methodology is to establish the design reference missions (DRMs) and the Objective Function. The design reference missions include detailed descriptions of the customer vehicles for the depot and their mission requirements, as well as the supplier that brings the fuel to the depot. Stated a different way, the research question asks, “Which architecture satisfies the Design Reference Missions (DRMs) for the least amount of liquid oxygen (LO2) and liquid hydrogen (LH2) consumed in flight or lost due to boiloff?” This implies the objective function will be a minimization function, and the individual terms in the function will be measurements of propellant consumption or loss.

After establishing the DRMs, we want to calculate the change in velocity (i.e.,  $\Delta v$ ) and the time-of-flight for a number of maneuvers in cislunar space. These values are calculated using restricted two-body techniques. The  $\Delta v$  values are then used to calculate propellant consumption. The rocket equation calculates how the fuel needed to accomplish the design reference mission tasks, as well as how much propellant the supplier will need to deliver propellant to the customer(s).

Calculating propellant tank sizes takes several steps. Initially, the rocket equation permits the calculation of a final mass of a vehicle, based on the initial dry mass, the specific impulse of its engine, and the  $\Delta v$  required. Subtracting the initial mass from the final mass gives the amount of propellant needed. The propellant mass is separated into the mass for liquid oxygen and the mass for liquid hydrogen, assuming a 6:1 oxidizer-to-fuel ratio.<sup>6</sup> Dividing the resulting masses of LO2 and LH2 by their respective densities gives the desired volumes of the fuel tanks.

Several tasks are involved to calculate expected losses of propellants due to boiloff. The first task is to characterize the thermal environment in which a given spacecraft must operate. This is done by calculating the heat load on the spacecraft in different orbits. The heat load consists of solar flux, reflected earth heating, and Earth-infrared heating. Second, these values are used to calculate the outside temperature of the spacecraft. Third, the outside temperature of the spacecraft and the size and configuration of the propellant tanks are used to calculate a boiloff rate. Fourth, the anticipated boiloff is calculated based on the length of time the spacecraft is exposed to that thermal environment – taken from the times of flight calculated for the individual maneuvers as described earlier. Boiloff losses are subtracted from the fuel volume. The amount of fuel remaining is compared to the amount of fuel required for the vehicle to perform the DRM.

The architecture with the smallest overall values for combined propellant consumption and loss ostensibly will be the “best” architecture. However, it is expected that there will be a number of lessons learned from the exercise. Some statistics will be computed – propellant losses as a percentage of propellant consumed for each vehicle, propellant losses as a percentage of the total propellant consumed, and propellant losses as a percentage of the total fuel shipped. It is expected that these statistics will also shed light on the “best” architecture.

### III. Candidate Architectures

#### A. Parameters Chosen

The vast majority of literature assumes the depot or depots would be supplied from the Earth. This study approaches the servicing of the depots from lunar-supplied resources. We focus on four factors as shown in Table 1.

1. Location of electrolysis and liquefaction processes: The Moon or the orbiting depot are considered. Of interest is the ease with which water (not a cryogen) could be shipped to the depot without suffering boiloff losses.
2. Location of the depot: low Earth orbit (LEO), geostationary orbit (GEO), the Earth-Moon Lagrange Point L1, and the lunar surface are considered.
3. Location of delivery to the customer: Generally speaking, this location is the depot except where the depot is on the Moon. If the depot is on the Moon, then direct transfer from tanker to customer vehicle would be required.
4. Method of fuel transfer: While the transfer of cryogenic fluids in microgravity has been studied, it has never been performed in space in any significant quantity.<sup>7</sup> This gives rise to the notion of bypassing the fluid transfer altogether by exchanging the fuel tanks, i.e., exchanging an empty tank for a full tank – much the same as is done with gas grills on the Earth.

Table 1. Architecture Defining Parameters and Potential Values

Parameter	Possible Values	Remarks
Location of depots	On Moon, L1, GEO, LEO	Locations most frequently mentioned in technical literature.
Location of electrolysis/liquefaction	On Moon, On-board orbiting depot	Electrolysis is performed daily in microgravity onboard the ISS. The technology is suitable for scaling.
Location of fuel transfer to customer	L1, GEO, LEO	Transfer at depot location. If the depot is located on the Moon, propellant transferred directly to customer vehicles at their location.
Method of fuel transfer	Bulk fuel (BF), Canister exchange (CX)	Canister exchange would require standardization of tank sizes and connecting hardware.

**B. Candidate Architectures Defined**

The candidate architectures developed are shown in Table 2. In the first third of the table, electrolysis is performed in orbit on the depot. Pure water from a lunar processing facility is shipped to the depot, and the depot can be located at L1, GEO, or LEO. Once the electrolysis and liquefaction has been accomplished, the depot stores the propellants until such time as they are transferred to the customer. There are two methods of transfer – bulk fluid or canister. The second third of the table is similar, except that electrolysis and liquefaction are performed on the Moon. The propellant is then shipped to the depot location for storage and distribution. In the bottom third of the table, electrolysis and liquefaction are performed on the Moon, but the propellants produced are also stored in a lunar depot. In this case, the propellants would be delivered directly from the Moon to the customer. Performing these functions on the Moon would likely take advantage of the abundant, but oblique, sunshine at the lunar poles.

Table 2. Candidate Architectures Defined

Location of processing	Location of depot	Location of transfer	Method of transfer	Remarks
In orbit	L1	L1	BF	Water is shipped from the lunar processing facility to the depot. Electrolysis and liquefaction take place on the depot.
In orbit	L1	L1	CX	
In orbit	GEO	GEO	BF	
In orbit	GEO	GEO	CX	
In orbit	LEO	LEO	BF	
In orbit	LEO	LEO	CX	
Moon	L1	L1	BF	Fuel is shipped from the lunar processing facility to the depot.
Moon	L1	L1	CX	
Moon	GEO	GEO	BF	
Moon	GEO	GEO	CX	
Moon	LEO	LEO	BF	
Moon	LEO	LEO	CX	
Moon	Moon	L1	BF	Electrolysis/fuel processing takes place on the Moon, and the depot is also on Moon. A tanker vehicle delivers fuel and oxidizer directly to the customer.
Moon	Moon	L1	CX	
Moon	Moon	GEO	BF	
Moon	Moon	GEO	CX	
Moon	Moon	LEO	BF	
Moon	Moon	LEO	CX	

**C. Initial Network Diagram**

Each of the candidate architectures shown in Table 3 represents a series of choices made – where to perform the electrolysis, where to locate a depot, where to transfer the propellants, and how to transfer the propellants. It is possible to depict these candidate architectures as separate paths from the Moon (the source of the propellants) to the final customers. Each architecture is represented by a unique path through the network, as shown in Fig. 2.

Node 1 is the processing facility on the Moon where excavated ice is melted and filtered and otherwise purified. Segments 1-2 and 1-3 represent the shipment of purified water to be loaded on tanker vehicles for transport to a depot for electrolysis and liquefaction. Segments 1-4 and 1-5 represent the shipment of LH2/LO2 to tankers to be delivered to an orbiting depot or delivered directly to customer vehicles. Nodes 6-11 represent depot locations where

electrolysis and liquefaction are performed on the depot. Nodes 12-17 represent propellant delivery to a depot. Nodes 18-23 represent direct delivery of propellant to the customer vehicle(s). Each segment shown involves the movement of fluid (either water or propellants) in the network and involves propellant consumption and propellant losses due to boiloff. These are calculated in the study and are presented later. Each candidate architecture can be described by the sequence of nodes, i.e., 1-2-6, 1-3-10, and so forth.

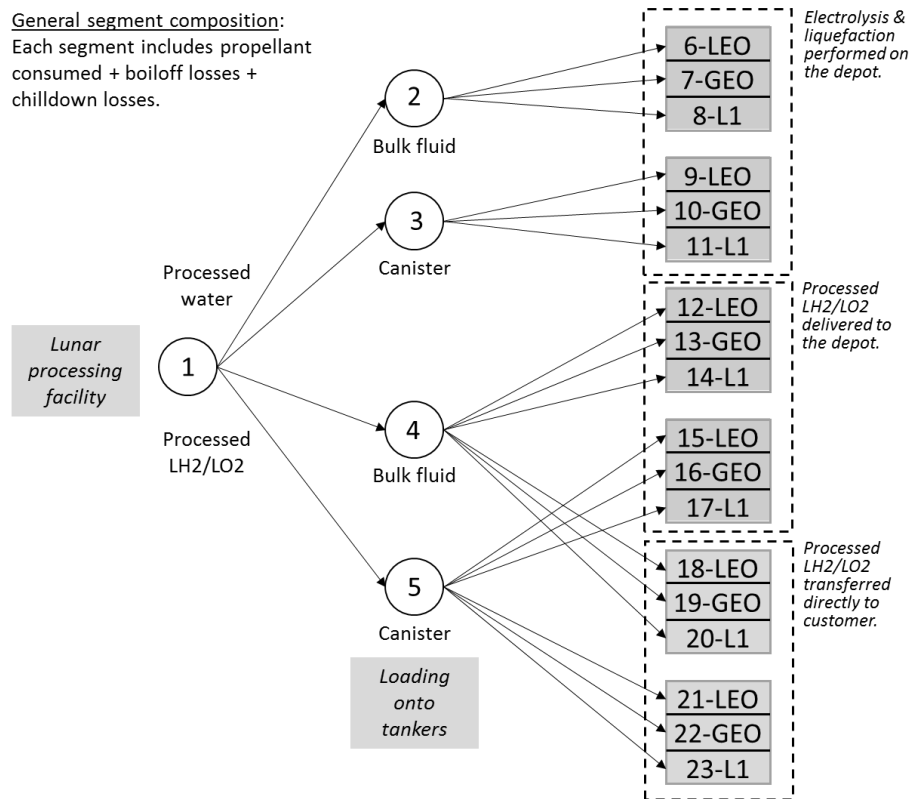


**Figure 2. Initial Architecture Network Diagram**

As noted on the diagram, each segment includes propellant consumed, propellant losses due to boiloff, and chilldown losses. Chilldown losses are incurred when transferring cryogenic propellant from one container to another. Some propellant is intentionally drained into the transfer pipe and allowed to boil off, thus cooling the pipe and preventing further losses during the transfer. This chilldown process is typically performed two times to chill the transfer pipe.<sup>‡</sup>

#### IV. Design Reference Missions

Design reference missions (DRM) are necessary to complete the candidate architectures and model the consumption and loss of propellant. Three DRMs are created, as described in Fig. 3. The first is a commercial satellite servicing (CSS) mission intended to supply hydrazine to satellite located in geosynchronous orbit. The second is a Government Mars Cargo mission intended to preposition cargo in orbit around Mars. Each of these design reference missions requires propellants to accomplish its tasks, and thus creates a demand on the architecture. A third DRM, the Propellant Delivery Mission, is created to supply the demand by transporting fuel, or water from the Moon to the depot or directly to the customer vehicle and is used to examine supply issues.

##### A. Commercial Satellite Servicing Mission

The amount of hydrazine on board a satellites limits the useful life of the satellite.<sup>8</sup> After the hydrazine is expended, the satellite is no longer able to alter its orbit or perform station-keeping. Many satellites must then be abandoned, since their high orbits (often in GEO) make them virtually inaccessible to a manned repair or salvage

<sup>‡</sup> P. McRight, personal communication, April 17, 2015.

mission. To minimize the clutter of old satellites in GEO, current practice boosts the nearly-expended satellite into a higher orbit, thus making room for a replacement.<sup>8</sup>

<p><u>Commercial Satellite Servicing Mission and Vehicle (CSSV)</u></p> <ul style="list-style-type: none"> <li>• Notional in-space vehicle; docked at the ISS; periodically resupplied with parts and hydrazine for satellite servicing.</li> <li>• Departs ISS, achieves GEO orbit, rendezvous with and services satellites, travels to and refuels at the depot, and returns to the ISS. Ten satellites per mission; one mission per month.</li> <li>• Dry mass: 4000 kg; Payload (robotic servicer): 500kg; Additional payload: 2000 kg N<sub>2</sub>H<sub>4</sub> (hydrazine); propellant capacity varies by depot location.</li> <li>• Powered by single RL10B-2 engine; I<sub>sp</sub> = 465.5 sec</li> <li>• Sizing based on available data for the proposed MacDonald-Dettwiler &amp; Associates satellite servicer.</li> </ul> <p><u>Government Mars Cargo Mission &amp; Vehicle (MCV)</u></p> <ul style="list-style-type: none"> <li>• Heavy lift vehicle to pre-position equipment and supplies in Mars orbit prior to crew arrival; based on Ares V Earth Departure Stage (EDS).</li> <li>• The mission assumes four vehicles; one vehicle launch every 6 months.</li> <li>• The MCV is initially launched into 200 km orbit. It docks with its cargo payload, rendezvous with the depot and refuels, and performs TMI.</li> <li>• Dry mass: 24,000 kg; Payload mass: 38,600–52,000 kg, depending on depot location.</li> <li>• Powered by single J2-X engine; I<sub>sp</sub> = 449 sec</li> <li>• Max fuel mass of 250,000 kg; 103,350 kg remains after initial launch into LEO.</li> </ul> <p><u>Propellant Delivery Mission &amp; Vehicle (LTV)</u></p> <ul style="list-style-type: none"> <li>• Notional lunar tanker vehicle (LTV).</li> <li>• Transports LO<sub>2</sub>/LH<sub>2</sub> or water to a fuel depot, or LO<sub>2</sub>/LH<sub>2</sub> directly to customer vehicles (CSSV or MCV), and returns to the Moon.</li> <li>• Flies as often as necessary to support demand.</li> <li>• Dry mass: 22,470 kg (20,000 kg structure + 2,470 kg engine)</li> <li>• Powered by single J-2X engine; I<sub>sp</sub> = 449 s; Thrust = 1,307 kN (294,000 lbf)</li> <li>• Using a 3:1 thrust-to-weight ratio, max takeoff weight = 268,071 kg*</li> </ul> <p>(* Fuel needed to fly to and from the depot or customer location reduces the allowable payload mass.)</p>
--

**Figure 3. Design Reference Missions**

This is the value of the Commercial Satellite Servicing Mission. Based at the International Space Station (ISS), the CSS mission uses an in-space vehicle (the Commercial Satellite Servicing Vehicle, or CSSV) with a LH2/LO2 engine. The vehicle carries a robotic payload, spare parts, tools, and hydrazine. Each month, the vehicle undocks from the ISS, achieves geostationary orbit, and rendezvous with and repairs or services ten satellites. The CSSV then flies to the depot and refuels, and returns to the ISS to receive new supplies and expendables, and then waits for the next mission. This DRM assumes one sortie every month.

The dry mass of the vehicle is 4,000 kilograms. The vehicle carries a robotic satellite servicer (500 kg) and carries 2,000 kg of hydrazine. The CSSV transfers 200 kg of hydrazine to each satellite serviced. The CSSV is powered by a single Aerojet Rocketdyne model RL10B-2 rocket engine. The engine has a specific impulse (vacuum) of 465.5 seconds and generates 24,750 pounds of thrust.<sup>9</sup>

## **B. Mars Cargo Mission**

The second DRM is a Government cargo mission to Mars. This DRM is adapted from NASA's Exploration Systems Architecture Study (ESAS).<sup>9</sup> The ESAS laid out NASA's plans for going back to the Moon and on to Mars. For the Mars mission, NASA planned to send four cargo vehicles to Mars which would arrive there in advance of the astronaut crew. The four vehicles would carry supplies, a Mars habitat, rovers, and anything else needed. Once the cargo vehicles had arrived safely, the astronauts would then follow in a separate crew vehicle.

The cargo vehicles themselves were the upper stage (Earth Departure Stage, or EDS) launched as a part of a heavy lift Ares V vehicle. Four Ares V rockets with EDS were to be launched over a period of 26 months to preposition supplies and equipment on Mars.<sup>9</sup> In the ESAS study, the EDS vehicles were assumed to be powered by

nuclear-thermal propulsion (NTP). Nuclear thermal propulsion has two advantages over chemical propulsion. It has a specific impulse ( $I_{sp}$ ) roughly double that of the best chemical engines – as much as 925 seconds -- yet overall much less mass. For the purposes of this study, however, the EDS configured for missions to the Moon is used instead. This EDS is powered by a single LH2/LO2 J-2X engine with an  $I_{sp}$  (vacuum) of 449 seconds.<sup>10</sup>

In the ESAS study, the heavy lift vehicle places the EDS and its payload into a 200 km/ 28.5 degree orbit.<sup>11</sup> The EDS docks with a lunar lander, and performs a trans-lunar injection from LEO. For the Mars Cargo DRM, the MCV is delivered to the same orbit as the EDS. The MCV docks with its cargo, maneuvers to the depot and refuels. Refueling at the depot enables the MCV to perform the trans-Mars injection (TMI) maneuver and the Mars Orbit Insertion upon arrival. Like the EDS, the MCV launches with 250,000 kg of propellant. After achieving LEO, the MCV has 103,500 kg of propellant remaining.<sup>12</sup>

### C. Propellant Delivery Mission

The Propellant Delivery Mission satisfies the need to deliver fuel and oxidizer (or water) to the depot, or directly to the CSSV or MCV. The mission is built around a fleet of unmanned vehicles, the Lunar Tanker Vehicles (LTV). It is powered by a J-2X engine, but has slightly less mass. As an in-space vehicle, the LTV is imagined as a rigid truss upon which necessary components (engine, fuel tanks, and so forth) are attached. The LTV is loaded with fuel, or water, and delivers its payload to the depot, or perhaps the other vehicles directly.

A thrust-to-weight ratio of 3 was used in determining maximum lift capacity of the LTV. When expressed in terms of Earth’s gravity, thrust-to-weight ratio ( $T/W_0$ ) for lunar or planetary landers in terms of Earth’s gravity of ~0.5 Earth’s gravity is commonly used.<sup>§</sup> (See also Sostaric and Merriam.)<sup>13</sup>

### D. Complete Architecture Network Diagram

With the addition of the CSSV and MCV, the network diagram is expanded in Fig. 4 to include the “supply side,” i.e., flights from the Moon using the LTV on the left as before, as well as delivery to the depot or customer vehicles in the center of the diagram. The nodes representing the CSSV and MCV have been added to the right hand side of the diagram.

### E. Objective Function

The network diagram enables development of an objective function, Eq.(1), with which the optimal delivery path, i.e., the architecture for which overall propellant loss and usage is minimized, may be identified. Terms for individual segments include propellant consumed by the respective vehicle, boiloff losses of the propellant for that vehicle, the boiloff losses of the propellant payload being delivered, as well as the chilldown losses related to propellant payload transfer.

With respect to the customer, consider segment 13-24 in which the CSSV vehicle receives bulk LH2/LO2 from the depot in GEO. For this segment, the CSSV departs its home base at the International Space Station (ISS), maneuvers from the ISS’ orbit to geostationary orbit. After doing so, it maneuvers to each of 10 satellites in GEO orbit and services them. It then maneuvers to the depot and refuels, then returns to the ISS. Each of its maneuvers requires the consumption of propellant, and during the entire time (including time spent at the ISS), it is subject to losing propellant to boiloff. And as with the transfer of propellants from the LTV to the depot, the transfer of propellants from the depot to the CSSV also includes a chilldown loss.

**Objective Function:** Minimize:  $X_{ijk} = P_{LTV} + B_{LTV} + B_{P/L} + C_{P/L} + P_{CSSV} + C_{CSSV} + B_{CSSV} + P_{MCV} + C_{MCV} + B_{MCV}$  (1)

where  $X_{ijk}$  maps to a unique candidate architecture (unique path in the network diagram), and

- $P_{LTV}$  = Propellant consumed by the LTV
- $B_{LTV}$  = Boiloff losses of the LTV’s own propellant
- $B_{P/L}$  = Boiloff losses for the LTV payload
- $C_{P/L}$  = Chilldown losses when transferring the LTV payload to the depot
- $P_{CSSV}$  = Propellant consumed by the CSSV
- $C_{CSSV}$  = Chilldown losses when the CSSV receives propellants
- $B_{CSSV}$  = Boiloff losses on the CSSV
- $P_{MCV}$  = Propellant consumed by the MCV
- $C_{MCV}$  = Chilldown losses when the MCV receives propellants
- $B_{MCV}$  = Boiloff losses on the MCV

---

<sup>§</sup> L. Kos, personal communication, August 11, 2015.



Recalling that the Commercial Satellite Servicing Vehicle (CSSV) delivers on a monthly basis, while the Mars Cargo Vehicle (MCV) launches once every six months, the objective function considers a six-month period in which there are six missions by the CSSV and one mission by the MCV. The number of supply missions flown by the LTV(s) will be based on the need for propellants. Since each candidate architecture will supply both the CSSV and MCV, each architecture will be designated by only three numbers, such as 1-3-10 or 1-4-19. This is done for convenience to shorten the architecture nomenclature. The delivery to the CSSV and MCV (delivery to nodes 24 and 25) is understood.

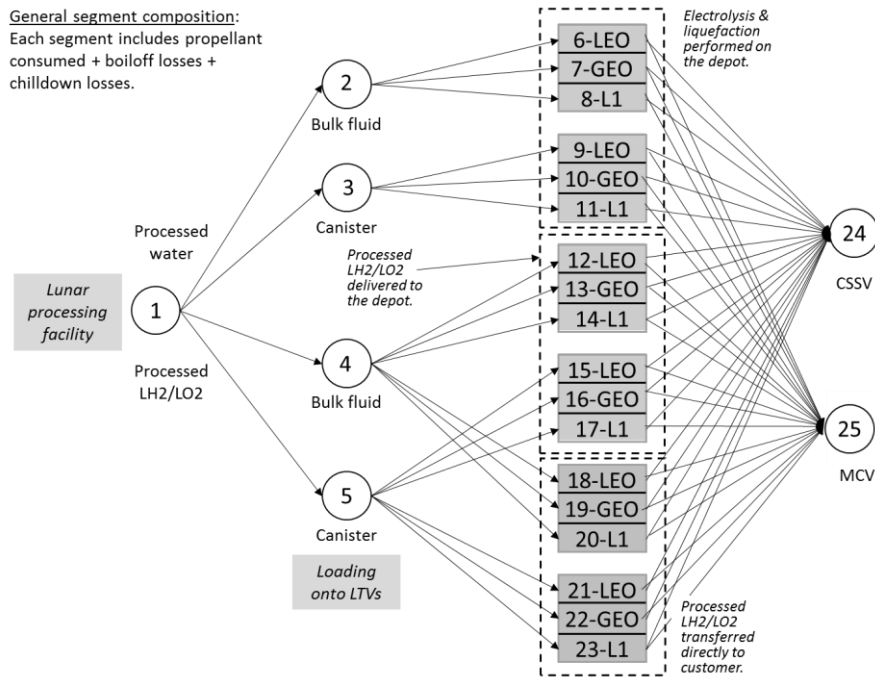


**Figure 4. Complete Architecture Network Diagram**

## V. Orbital Mechanics

Restricted two-body techniques were used for simplification as described in Fig. 1. For the CSSV performing co-orbital rendezvous to service satellites in GEO, the ten customer satellites were assumed to be evenly distributed 36 degrees apart. For the CSSV or MCV performing a co-orbital rendezvous with a depot in GEO, the depot was assumed to be 180 degrees ahead, i.e., worst case. The LEO orbit for the depot was assumed to be 400 km altitude, 0 degrees inclination.

As described in the previous section, each segment on the network diagram represents multiple activities, whether the LTV in delivering propellants, the CSSV servicing satellites and then refueling, or the MCV docking with its payload and maneuvering to the depot to refuel before executing trans-Mars-injection (TMI). An incremental approach is used in that the  $\Delta v$  and time-of-flight values were first calculated for individual maneuvers, e.g., ISS to GEO, rendezvous in GEO, etc. These values for mission segments are provided in Table 3.

Table 3. Delta-v and Time-of-Flight Values for Individual Maneuvers

Maneuver	Description	Delta-v (km/s)	Time-of-Flight (hrs)
Depot in LEO (400 km altitude, 0 deg inclination)			
GEO-to-LEO	CSSV rendezvous with depot in LEO	3.854	5.3
Co-orbital rendezvous in LEO	CSSV or MCV rendezvous with depot in LEO	2.031	2.3

ISS to GEO	CSSV to GEO with plane change	4.838	5.3
GEO co-orbital rendezvous (10)	CSSV rendezvous with 10 satellites	2.320	215.4
LEO to ISS	CSSV return from depot at LEO to ISS	6.683	0.8
LEO (200 km/28.5 deg) to LEO	MCV from initial orbit to depot	3.889	0.8
LEO-to-Mars	MCV departing LEO enroute to Mars	5.670	288 days
Moon-to-LEO	LTV deliver to depot at LEO	6.287	119.6
LEO-to-Moon	LTV return to Moon from LEO	6.287	119.6
Depot in GEO			
ISS-to-GEO	CSSV to GEO to service satellites	4.838	5.3
GEO co-orbital rendezvous (10)	CSSV rendezvous with 10 satellites	2.320	215.4
Co-orbital rendezvous in GEO	Rendezvous with depot in GEO	1.905	12.0
GEO-to-ISS	CSSV return from GEO to ISS	4.839	5.3
LEO (200 km/28.5 deg)-to-GEO	MCV goes to GEO to refuel at depot there	4.291	5.3
GEO-to-Mars	MCV departing GEO enroute to Mars	4.278	288 days
Moon-to-GEO	LTV delivers fuel to GEO	3.995	136.1
GEO-to-Moon	LTV returning to Moon after delivery to GEO	3.999	136.1
Depot at L1			
ISS-to-GEO	CSSV to GEO to service satellites	4.838	5.3
GEO co-orbital rendezvous (10)	CSSV rendezvous with 10 satellites	2.320	215.4
GEO-to-L1	CSSV going to L1 to refuel	1.332	107.4
L1-to-ISS	CSSV returning to ISS after refueling at L1	3.811	92.2
LEO (200 km/28.5 deg)-to-L1	MCV going to L1 to refuel	3.780	92.1
L1-to-Mars	MCV departing L1 enroute to Mars	4.327	288 days
Moon-to-L1	LTV delivering fuel to L1	2.342	65.6
L1-to-Moon	LTV returns to Moon from L1	2.342	65.6

Delta-v and TOF for the transfer vehicles as a function of depot location are provided in Table 4. The time of flight for travel to Mars was based on “conjunction class” trajectories where the Earth at launch and Mars at arrival are nearly in direct opposition. Nine such launch opportunities from the year 2002-2011 are recorded in the NASA’s Interplanetary Mission Design Handbook.<sup>14</sup> The mean  $\Delta v$  and TOF are 3.673 km/sec and 288 days, respectively.

The delta-v values suggest that LEO is the most stressing depot location for all three DRM vehicles. Likewise, L1 is the least stressing depot location for all three DRM vehicles, although the increased TOF for the CSSV and MCV also increases boiloff mass.

Table 4. Summary of Delta-v and Time of Flight (TOF)

Depot/LTV Location	Delta-v (km/s)	TOF (hrs)
Commercial Satellite Servicing Vehicle (CSSV)		
Depot or LTV in LEO	17.695	226.7
Depot or LTV in GEO	13.902	237.9
Depot or LTV at L1	12.301	420.3
Mars Cargo Vehicle (MCV)		
Depot in LEO or tanker delivers to LEO	9.559	24.75 + travel to Mars (288 days) <sup>1</sup>
Depot in GEO or tanker delivers to GEO	8.569	29.26 + travel to Mars (288 days) <sup>1</sup>

Depot at L1 or tanker delivers to L1	8.107	116.1 + travel to Mars (288 days) <sup>1</sup>
Lunar Tanker Vehicle (LTV)		
Depot in LEO	14.605	241.5
Depot in GEO	9.899	284.3
Depot in L1	4.684	131.3
<sup>1</sup> Includes 24 hours spent in LEO after launch		

## VI. Fuel Consumption and Propellant Delivery

For each vehicle, a backwards planning approach was used. To illustrate, the simplest case among all three vehicles was for the lunar tanker vehicle (LTV) delivering fuel to the depot located at L1. That is, the first question asked was “How much fuel will be needed to fly the [empty] LTV back to the Moon after it makes its delivery?” Once that mass of fuel was determined, that mass together with the dry mass of the vehicle and the payload mass became the  $m_{\text{final}}$  used in the next iteration of the rocket equation. The next  $m_{\text{initial}}$  calculated represented total vehicle mass – dry mass, payload mass, fuel to maneuver to L1, and the fuel to maneuver the empty LTV back to the Moon.

For the Commercial Satellite Servicing Vehicle (CSSV) a similar approach was used. Recall that the CSSV starts its mission at the International Space Station. It maneuvers to GEO, and rendezvous with and services ten different satellites. It transfers 200 kg of hydrazine to each satellite. It then maneuvers to the depot and refuels, and returns to the ISS and receives a new payload (2,000 kg) of hydrazine.

The fuel consumption calculations for MCV were similar to those for the CSSV, with the exception that the MCV starts out in LEO with 103,350 kg of propellant remaining after launch.<sup>10</sup> So the initial step with MCV was to determine the maximum payload mass that would still allow the MCV to fly to the depot location with the remaining propellant. (After the arrival at the depot, the initial propellant from the launch is assumed to be fully consumed.) Once that payload was determined, the payload mass and the MCV dry mass become the  $m_{\text{final}}$  that must be delivered to Mars orbit.

For the LTV calculations, the same backward planning process was used as with the other vehicles. However, for the LTV the payload is not known in advance. It follows that the amount of propellant the LTV consumes to make the trip reduces that portion of the vehicle lift capacity that can be allocated to the payload, and several iterations of the rocket equation may be needed until the right combination of fuel and payload are achieved.

Table 5 summarizes the fuel consumption and maximum permissible for each vehicle for each of the proposed depot locations. It can be seen that LEO is the most severe location for the depot, while L1 is the least severe. Low Earth orbit is not a viable location for a depot supplied from lunar resources, unless some means is used to reduce the  $\Delta v$  requirement. It is also evident that propellant delivery to geostationary orbit is a poor choice, where the LTV consumes much more propellant than it is able to deliver. At L1 the LTV still uses more propellant than it delivers, but almost achieves parity. Of the three orbit locations examined, L1 is clearly the most efficient location to deliver propellant.

Table 5. Summary of Fuel Consumption and Maximum Permissible Payloads

Depot Location	Fuel Required (kg)	Maximum Payload (kg)
Commercial Satellite Servicing Vehicle (CSSV) <sup>1</sup>		
LEO	243,621	2,000
GEO	110,229	2,000
L1	77,803	2,000
Mars Cargo Vehicle (MCV) <sup>2</sup>		
LEO	191,075	48,850
GEO	102,740	38,600
L1	126,978	52,000
Lunar Tanker Vehicle (LTV)		

LEO	571,796 <sup>3</sup>	---
GEO	231,065	14,520
L1	126,320	119,275

<sup>1</sup> CSSV fuel is that needed for one mission – departing from the ISS, servicing satellites, refueling, and returning to the ISS.

<sup>2</sup> MCV fuel is that needed to depart LEO and refuel at the depot, perform TMI, and have enough fuel remaining to enter Martian orbit. The fuel remaining after achieving initial LEO orbit limits the payload that can be taken forward.

<sup>3</sup> LTV fuel required to deliver in LEO is greater than its total lift capacity.

An additional implication of these findings relates to the sizing of the depot. The DRMs for the CSSV and MCV calls for depot visits of once each month and once every sixth month, respectively. These requirements and schedules thus define the depot capacity needed. The size of the depot at each location would be the sum of propellant mass needed by the CSSV and the mass needed by the MCV, since in the sixth month, both vehicles would maneuver to the depot to obtain propellant (Table 6). It can be seen that, depending on the location, the suggested depot size varies considerably. If it were feasible to supply a depot in LEO from the Moon, the depot would need to be more than double the size of a depot at L1.

Table 6. Fuel Depot Sizing

Depot Location	CSSV Fuel Required (kg)	MCV Fuel Required (kg)	Suggested Depot Size/Remarks
LEO (400 km/0 deg)	243,621 (once per month)	191,075 (once every 6 mos.)	434,696 kg, based on fueling both vehicles every 6th month, but the LTV cannot service the depot in LEO.
GEO	110,229 (once per month)	102,740 (once every 6 mos.)	212,969 kg, based on fueling both vehicles every 6th month.
L1	77,803 (once per month)	126,978 (once every 6 mos.)	204,871 kg, based on fueling both vehicles every 6th month.

An additional implication relates to throughput, i.e., the quantity of fuel passing through the depot over a six month period. How throughput as a function of depot location relates to LTV sorties is presented in Table 7. To support a depot at L1, the LTV delivers almost as much as it consumes. Likewise, fuel consumption requirements for the CSSV and the MCV are the least for the depot at L1, resulting in a smaller depot and smaller throughput over a six month period.

Table 7. LTV Flights to Supply the Depot

Depot Location	Mass Required per Six Months (kg)	Mass LTV can deliver per flight (kg)	LTV Flights needed to service the depot
LEO <sup>1</sup>	1,653,401	---	---
GEO	764,114	14,520	52.625 →53
L1	593,796	119,275	4.978 →5 <sup>2</sup>

<sup>1</sup>LTV cannot support a depot located in LEO.

<sup>2</sup>Bulk fuel only. Canisters require 6 flights.

Eliminating low Earth orbit (400 km altitude, 0 degrees inclination) as a viable location narrows the range of feasible solutions. Furthermore, since it is impractical to service the CSSV or MCV directly in GEO, other segments also become infeasible. As shown in Fig. 5, ten paths remain for evaluation in greater detail.

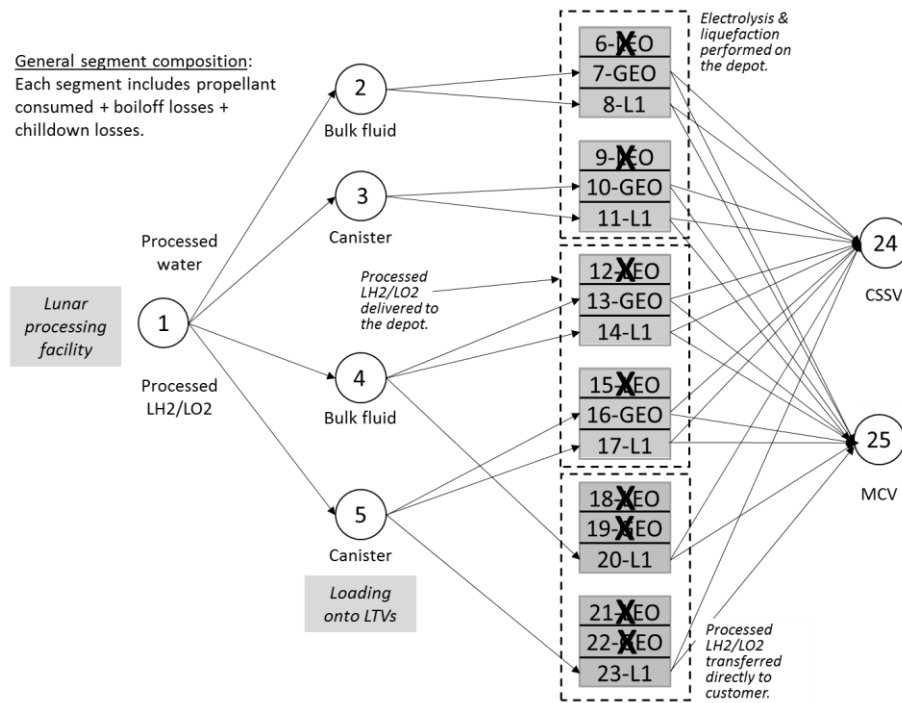


**Figure 5. Updated Architecture Network Diagram**

## VII. Propellant and Payload Losses

### A. Boiloff Losses

As a precursor to determining propellant losses, the thermal environment of the spacecraft must be characterized. Determination of the temperature of the external surface of the spacecraft, along with the propellant tank size and shape and other factors allows estimation of the boiloff rate.

For spacecraft in Earth orbit, the thermal environment consists of three external sources of heat– energy from the Sun (solar flux), Earth-reflected heating (albedo times the incident solar flux), and Earth-emitted radiation, also called Earth infrared radiation, or simply Earth-IR. At geostationary orbit (GEO), the values for Earth reflected heating and earth-IR decrease substantially. At Earth-Moon L1, the values for Earth reflected heating and Earth-IR are almost non-existent. Some thermal analysts ignore the effects of Earth reflected heating and Earth-IR at GEO and L1 but they are included here to be consistent.\*\*

From Thornton, environmental heating rates depend on altitude and orientation of the spacecraft with respect to sources of heat.<sup>15</sup> The solar heat received by the spacecraft surface ( $q_s$ ) is given by Eq. (2):

$$q_s = 1,367 a_s \cos \psi \quad (2)$$

where  $a_s$ , is the surface absorptivity and  $\psi$  is the angle between the solar flux vector and the surface normal.<sup>14</sup> The solar constant is 1,367 W/m<sup>2</sup> at 1 AU. Surface absorptivity is set conservatively as  $a_s = 1$ . Conservatively assuming the spacecraft normal to the Sun and the Earth and Moon as coplanar with the Sun such that  $\psi = 0$  degrees, leaves cosine of  $\psi = 1$ .

The radiation emitted by the Earth (Earth-infrared) can be approximated by assuming the Earth to be a blackbody radiating at  $T_e = 289$  K. The radiation absorbed by the (spacecraft) surface can be expressed as Eq. (3):

\*\* S. Sutherland, personal communication, April 22, 2015.

$$q_e = \sigma T_e^4 a_e F \quad (3)$$

where  $\sigma$  is Boltzmann's Constant  $5.67051 \times 10^{-8} \text{ W m}^{-2} \text{ K}^{-4}$   
 $a_e$  is the surface absorptivity for Earth-infrared radiation, and  
 $F$  is the view factor.

The view factor, Eq. (4), (also called the shape factor or configuration factor) describes the fraction of the radiant energy that arrives at the surface.<sup>15</sup>

$$F = \cos \lambda / H^2 \quad (4)$$

where  $\lambda$  = the angle between the surface normal and the heat flux  
 $H = r/R$ , where  $R$  is radius of the Earth, and  $r$  is the distance from the center of the Earth to the spacecraft

Surface absorptivity is conservatively set to 1. The spacecraft surface normal points to the center of the Earth; the angle  $\lambda$  is zero degrees, and the cosine is 1. Thus, the view factor  $F$ , Eq. (5), becomes

$$F = 1/H^2 \quad (5)$$

Earth reflected heating, Eq. (6), depends on the albedo factor (AF), and is defined as the fraction of the solar radiation striking the Earth that is reflected back into space. Earth reflected heating is described by

$$q_a = 1,367 \text{ AF } a_s F \cos \theta \quad (6)$$

where  $\theta$  is the reflection angle from the Earth to the spacecraft. Using an average Earth albedo (AF) of 0.367 per NASA/Jet Propulsion Laboratory.<sup>16</sup> Again, conservatively setting surface absorptivity is at 1, and  $\theta =$  zero; so that the expression reduces to  $q_a = 1,367 (0.367) (F)$ . Thus, the expressions for solar flux, Earth infrared radiation, and Earth reflected heating are:

Solar flux = 1,367 Watts/meter<sup>2</sup> (for all locations)  
 Earth infrared =  $\sigma T_e^4 F$ , where  $T = 289 \text{ K}$ , and  $F = 1/H^2 = (R/r)^2$ , and  
 Earth reflected heating = 1,367 (0.367) (F), where  $F = 1/H^2 = (R/r)^2$

The values calculated for all sources are summarized in Table 8.

Table 8. Thermal Environment at LEO, GEO, and L1

Heat (Watts/m <sup>2</sup> )	LEO	GEO	L1
Solar constant	1,367	1,367	1,367
Earth emitted infrared	350.3	9.1	0.16
Earth reflected heating	444.2	11.5	0.20
Total <sup>1</sup>	2,161.5	1,387.6	1,367.36

<sup>1</sup> This represents the energy deposited on the cross section of the spacecraft propellant tanks.

Tanks are sized appropriate to the required propellant load. For simplicity, spherical tanks are assumed for propellant and canister tanks, except for the MCV where cylindrical tanks are envisioned for bulk fuel transport. Table 9 summarizes the estimates of the dimensions of these tanks.

Table 9. Estimated Dimensions of Propellant Tanks

Delivery	Delivery	LTV Propellant	LTV Payload	CSSV	MCV
----------	----------	----------------	-------------	------	-----

Location	Method				
GEO	BF	LH2: 4.80 m LO2: 3.41 m	LH2: 1.91 m LO2: 1.36 m	LH2: 3.75 m LO2: 2.66 m	LH2: 10 x 6.36m LO2: 10 x 2.29m
	CX	LH2/LO2: 1.35 m			
L1	BF	LH2: 3.92 m LO2: 2.79 m	LH2: 3.85 m LO2: 2.73 m	LH2: 3.34 m LO2: 2.37 m	LH2: 10 x 6.41m LO2: 10 x 2.29m
	CX	LH2/LO2: 1.35 m			

Given the thermal environment and the illuminated area of the tank, the surface temperature can be estimated. Adapting the expression Eq. (7) from Wertz and Larson<sup>17</sup> for Earth reflected heating and Earth infrared yields expression Eq. (8).<sup>††</sup> Simplifying yields Eq. (9).

$$\sigma T^4 = (\alpha/\varepsilon)(S) \times (A_p/A) \quad (7)$$

$$\sigma T^4 = [(1/\varepsilon)(\alpha(S+RH) + \varepsilon(E))] \times (A_p/A) \quad (8)$$

$$\sigma T^4 = [(\alpha/\varepsilon)(S) + (\alpha/\varepsilon)(RH) + E] \times (A_p/A) \quad (9)$$

where T = outside temperature of the spacecraft (K)  
 $\sigma$  = Boltzmann's constant =  $5.67051 \times 10^{-8} \text{ W/m}^2 \text{ K}^{-4}$   
 $\alpha$  = absorptivity (= 0.14 for outer layer of MLI)  
 $\varepsilon$  = emissivity (= 0.60 for outer layer of MLI)  
S = solar flux (1,367 W/m<sup>2</sup>)  
RH = Earth reflected heating  
E = Earth infrared  
 $A_p$  = projected area of the propellant tank  
A = total surface area of the propellant tank

The propellant tanks for the various spacecraft (CSSV, MCV, and LTV) are not enclosed but rather are exposed to space, except for layers of multi-layer insulation (MLI). The values for absorptivity and emissivity used are based on the recommendations of the Advanced Concepts Office at NASA/Marshall Space Flight Center<sup>††</sup> and correspond to the specifications of Sheldahl Aluminum-coated (one side) Fluoro ethylene propylene (FEP).<sup>18</sup>

The estimated surface temperatures of respective propellant tanks are given in Table 10. The differing values for the LH2 and LO2 tanks of the MCV stem from the difference in length of the two tanks. The value of  $A_p/A$  for the (longer) LH2 tank is 0.1781, while the value for the LO2 tank is 0.1.  $A_p/A$  for all spherical tanks is 0.25.

Table 10. Estimated Surface Temperatures for Propellant Tanks

Location	Surface Temperature for All Spherical Tanks for CSSV, MCV, LTV (K)	Surface Temperature for Bulk Propellant Tanks for MCV (K)
LEO	242	LH2: 222 LO2: 192
GEO	195	LH2: 180 LO2: 155
L1	194	LH2: 178 LO2: 154

<sup>††</sup> S. Sutherlin, personal communication, April 22, 2015.

<sup>‡‡</sup> S. Sutherlin, personal communication, April 22, 2015.

The Modified Lockheed Model<sup>19</sup>, Eq. (10), considers three heat transfer mechanisms i.e., solid conduction, radiation between blanket layers, and gas conduction, and yields the rate (q) of heat transfer through the layers of insulation into the fuel tank in W/m<sup>2</sup>.

$$q = 0.00024*(0.017+7E-6(800-T) +0.0228*\ln(T))*(N^*)^{2.63}(T_h-T_c)/N_s + 4.944E-10*\epsilon*(T_h^{4.67}-T_c^{4.67})/N_s + 1.46E4*P*(T_h^{0.52}-T_c^{0.52})/N_s \quad (10)$$

where: q = heat transfer rate in W/m<sup>2</sup>  
 $\epsilon$  = emissivity of the inner layers of MLI (here = 0.035)  
 $T_h$  = temperature on outside tank surface (K)  
 $T_c$  = propellant temperature (20 K for LH2, 80 K for LO2)  
 $T$  =  $(T_h+T_c)/2$   
 $N^*$  = number of layers/cm of MLI  
 $N_s$  = number of layers of MLI, and  
 $P$  = pressure between the layers of MLI (Torr)

Sixty layers of MLI are assumed. For 60 layers, the rate of cryogenic boiloff stabilizes to approximately 0.5 – 1.0% per month for LO2, and approximately 2.5 – 5.0% per month for LH2.<sup>20</sup> A density of the MLI blankets of 10 layers per centimeter is assumed. Inner layers of low emissivity MLI, e.g., Aluminum-coated (two sides) polyethylene terephthalate (PET, commonly known as Mylar),<sup>18</sup> with an emissivity of 0.035, are used.<sup>§§</sup> Table 11 provides the estimated range of boiloff rates across all tank configurations for each location.

### B. Chilloff Losses

Because the heat of the pipe will cause the cryogen to boil, the pipe through which the cryogen will move must be chilled to reduce losses.<sup>\*\*\*</sup> Typically the transfer pipe is partially filled with the cryogen so that it boils and cools the pipe. This action is repeated to complete the cooling. Then the planned fluid transfer can be initiated. The two partial releases into the transfer pipe equate to having filled the pipe completely one time. So, the chilloff loss is

Table 11. Estimated Range of Boiloff Rates Across All Tank Configurations

Cryogen	Boiloff Rate at Location (kg/hr)		
	LEO (400 km)	GEO	L1
LH2	0.0164 - 0.2044	0.0097 – 0.1268	0.0095 – 0.1245
LO2	0.0296 – 0.1437	0.0157 – 0.1002	0.0153 – 0.0977

1. Based on Modified Lockheed Model  
2. Assumes 60 layers of multi-layer insulation (MLI)  
3. Solar constant, Earth-reflected heating, and Earth-infrared radiation included for each orbit.

considered to be the volume of the pipe times the density of the cryogen. This loss would be incurred for every transfer.

For the study effort, the dimensions for a transfer pipe were selected as diameter of 0.1 meters and length of 10 meters. For liquid hydrogen, the estimated chilloff loss is:

$$\text{Chilloff loss}_{LH2} = 0.0785 \text{ m}^3 \times 70.99 \text{ kg/m}^3 = 5.57 \text{ kg per transfer.}$$

Likewise, for liquid oxygen, the chilloff loss is estimated as:

$$\text{Chilloff loss}_{LO2} = 0.0785 \text{ m}^3 \times 1911.6 \text{ kg/m}^3 = 93.6 \text{ kg per transfer}$$

### C. Boiloff and Chilloff Loss Compilation

<sup>§§</sup> S. Sutherlin, personal communication, May 7, 2015.

<sup>\*\*\*</sup> P. McRight, personal communication, April 17, 2015.



Losses due to chilldown and boiloff are compiled across the feasible mission architectures. For segments in which a vehicle is moving from one orbit to another, such as the LTV delivering fuel to geostationary orbit, the boiloff rate used was for that region in which the preponderance of the time of flight occurred. Thus, for the LTV delivering fuel to GEO, the boiloff rates for L1 were applied. For the CSSV refueling at L1, boiloff rates for all three orbits were used. The LEO rate was used when the CSSV was idle at the ISS. The GEO rate was used when servicing satellites. And, the L1 rate was used when maneuvering to L1, i.e., beyond GEO. For the MCV, the LEO rate was used in LEO, the GEO rate was used if maneuvering to GEO to refuel, and the L1 rate used for the transit to Mars. As will be seen, the loss of propellant through boiloff and chilldown is negligible relative to the propellant loads envisioned.

### **VIII. Mission Architecture Comparison**

The propellant consumption and losses of the candidate architectures are presented in Table 12 in the terms of the objective function Eq. (1). The strongest finding is that not only do the architectures which position the depot at L1 require the least amount of total propellant but that the propellant requirements are an order of magnitude less than for those architectures involving a depot at GEO. For flights to L1, the bulk fuel method of transfer is preferred. Even though chilldown losses are incurred by this method, the smaller surface area of the bulk fuel tanks results in less boiloff than for canister exchange. However, for deliveries to GEO, the increased boiloff seen with canister exchange is exceeded by the chilldown losses when a large number of LTV flights is involved, each of which involves chilldown losses when transferring from the LTV to the depot.

As depicted in Fig. 6, the architecture which satisfies the Design Reference Missions (DRMs) for the least amount of liquid oxygen (LO<sub>2</sub>) and liquid hydrogen (LH<sub>2</sub>) consumed in flight or lost due to boiloff is Architecture 1-2-8, in which bulk water is shipped to a depot at L1, and electrolysis and liquefaction would be performed at the depot. This architecture requires less  $\Delta v$  than shipping to a depot in GEO. Shipping in bulk takes advantage of the smaller total surface area of bulk propellant tanks versus that for combined canister tanks. Finally, shipping water to the depot avoids any losses of payload to boiloff during the flight, as well as any chilldown losses between the LTV and the depot. However, it should be noted that while architecture 1-2-8 uses the least resources it may not be optimal given that processing the water into liquid hydrogen and liquid oxygen at the depot would require large amounts of electric power, thereby increasing its size, complexity, construction cost, and operating costs. However, the amount of power necessary to perform electrolysis and liquefaction (either on the Moon or on a depot) was not calculated for this effort.

Table 12. Propellant Consumption and Loss by Candidate Architecture

Candidate Architecture (Path)	LTV Fuel Consumed ( $P_{LTV}$ )	LTV Boiloff Losses ( $B_{LTV}$ )	LTV P/L Boiloff ( $B_{P/L}$ )	LTV Chilldown Losses ( $C_{P/L}$ )	CSSV Fuel Consumed ( $P_{CSSV}$ )	CSSV Chilldown Losses ( $C_{CSSV}$ )	CSSV Boiloff Losses ( $B_{CSSV}$ )	MCV Fuel Consumed ( $P_{MCV}$ )	MCV Chilldown Losses ( $C_{MCV}$ )	MCV Boiloff Losses ( $B_{MCV}$ )	Architecture Total Propellant (kg)
1-2-8 BF H2O L1	631,600	96	0	0	466,818	596	616	126,978	99	1,450	1,228,254
1-4-14 BF Prop L1	631,600	96	55	596	466,818	596	616	126,978	99	1,450	1,228,905
1-5-17 CX Prop L1	673,551	115	118	0	466,818	0	1,528	126,978	0	3,096	1,272,203
1-3-11 CX H2O L1	676,554	115	0	0	466,818	0	1,528	126,978	0	3,096	1,275,088
1-4-20 BF DD L1	715,005	96	74	0	466,818	595	616	126,978	198	1,450	1,311,830
1-5-23 CX DD L1	769,129	134	150	0	466,818	0	1,528	126,978	0	3,096	1,367,832
1-2-7 BF H2O GEO	12,246,445	3,288	0	0	661,374	596	743	102,740	99	1,432	13,016,719
1-5-16 CX Prop GEO	12,246,445	3,288	352	0	661,374	0	1,937	102,740	0	2,445	13,018,582
1-4-13 BF Prop GEO	12,246,445	3,288	278	5,258	661,374	596	738	102,740	99	1,432	13,022,248
1-3-10 CX H2O GEO	16,227,386	4,591	0	0	661,374	0	1,937	102,740	0	2,445	17,000,474
BF = Bulk Fuel   CX = Canister Exchange   Prop = Propellants   H2O = Water   DD = Direct Delivery											

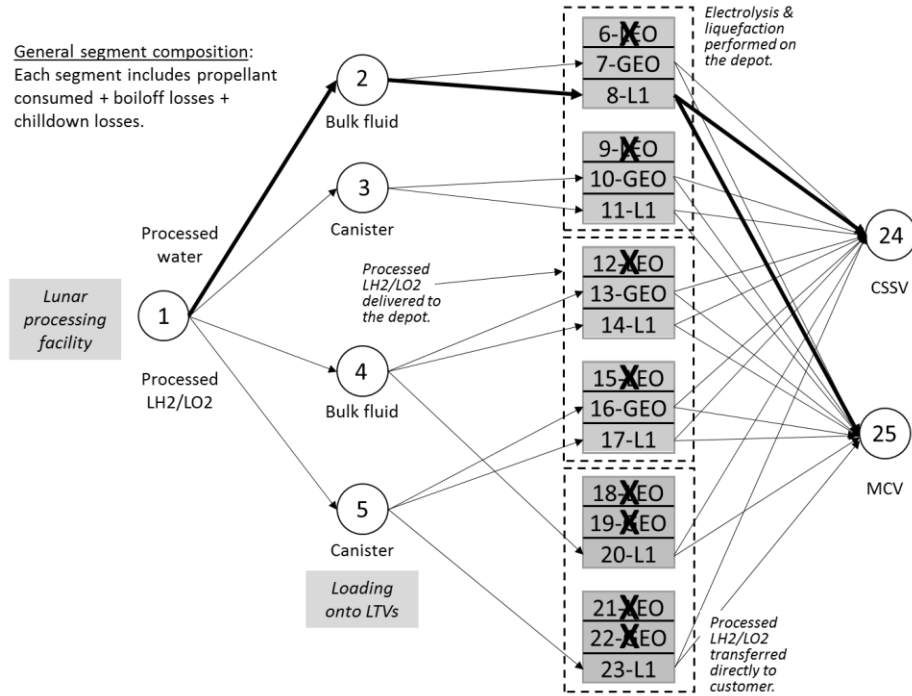


**Figure 6. Final Network Architecture Diagram**

The impact of losses was negligible for all architectures as shown in Table 13. Boiloff as a percentage of total fuel consumed ranged from 0.047% - 0.286%. The smallest percentage of losses as a percentage of propellant consumed was for the depot location in GEO, where the largest amount of propellant was consumed (fraction is smaller because denominator is larger). The largest percentage of losses as a percentage of propellant consumed was for depot locations at L1. Boiloff as a percentage of total fuel shipped ranged from 0.481% - 1.530%. The smallest percentage occurred for shipments to L1, where the fuel shipped was the least, and the fuel losses were smaller. The larger percentages were almost exclusively for shipments to GEO, where the mass of propellant shipped was greater, but the losses were greater as well.

Two sensitivity analyses were undertaken with this study. The first of these examined adding a second engine to the LTV. Adding a second engine to the LTV increased the payload and, thereby reduced the number of sorties required to service the depot or customer vehicles. Transfer losses were also reduced. Overall fuel consumption remained much the same as for the single-engine LTV. These trends served to underscore the L1 solution.

The other sensitivity analysis examined the relationship between MLI mass and predicted boiloff. While the main study used 60 layers of MLI, 30 layers of MLI were chosen for investigation, and two specific architectures – Architecture 1-4-14 (the delivery of bulk fuel to a depot at L1) and Architecture 1-5-17 (the delivery of propellant in canisters to a depot at L1) – were chosen as the focus of the calculations.

For each architecture, there was an expected increase in boiloff losses. However, for both architectures considered the reduction in MLI mass was roughly double the increase in the mass lost to boiloff. This suggests that further investigation is needed to determine the “right” amount of MLI to balance expected boiloff with overall spacecraft mass.

In addition, the total propellant consumption and losses for architectures 1-4-14 and 1-5-17 were 1,231,104 kg and 1,277,059 kg, respectively. Even with the increase in boiloff losses, roughly double that for 60 layers of MLI, boiloff accounted for less than one percent of the total consumption and losses for each architecture. Cryogenic propellant boiloff, while a concern, does not appear to be a deciding factor in the choice of architectures.

Table 13. Propellant Loss Statistics

Candidate Architecture	LTV losses % of fuel	CSSV losses % of fuel	MCV losses % of fuel	Boiloff % of fuel	Boiloff % of fuel
------------------------	-------------------------	--------------------------	-------------------------	----------------------	----------------------

	consumed	consumed	consumed	consumed	shipped
1-2-8 BF H2O L1	0.015%	0.260%	1.220%	0.233%	0.481%
1-4-14 BF prop L1	0.015%	0.260%	1.220%	0.286%	0.591%
1-5-17 CX prop L1	0.015%	0.327%	2.438%	0.364%	0.821%
1-3-11 CX H2O L1	0.016%	0.327%	2.438%	0.357%	0.798%
1-4-20 BF DD L1	0.013%	0.260%	1.298%	0.231%	0.510%
1-5-23 CX DD L1	0.017%	0.327%	2.438%	0.360%	0.826%
1-2-7 BF H2O GEO	0.027%	0.203%	1.491%	0.047%	0.806%
1-5-16 CX prop GEO	0.027%	0.293%	2.380%	0.062%	1.050%
1-4-13 BF prop GEO	0.027%	0.202%	1.491%	0.090%	1.530%
1-3-10 CX H2O GEO	0.028%	0.293%	2.380%	0.053%	1.174%

## IX. Conclusions

Of the potential methods discussed for judging the goodness of candidate architectures, calculating fuel consumption and losses gives the greatest credible insight into potential fuel depot operations. This is because the supporting tools – orbital mechanics, space vehicle design, thermal analysis, boiloff calculation, and others -- are well established.

Earth-Moon L1 is the best location for an orbiting depot. Because of the reduced  $\Delta v$  requirements, supplying a depot at L1 provides the most fuel for the least cost (in fuel consumption and losses) to transport it.

Low Earth Orbit is not a viable location for a depot supplied from the Moon. The fuel required for the tanker vehicle to fly round trip to a depot in LEO far exceeds the lift capacity of the vehicle. Even if the propellant needed was within the vehicle lift capacity, propellant delivered would be a small fraction of that consumed.

Boiloff would not be the primary factor in choosing among competing architectures. For fuel tanks with 60 layers of MLI, propellant boiloff did not result in crippling losses of propellant, even for the transit to Mars. This suggests that so-called zero boiloff (ZBO) technologies, such as cryocoolers, may not be required for these vehicles. Carrying more fuel is the more simple solution.

The payload capacity of the MCV is not limited by its propellant mass, but by the propellant mass remaining after launch. The fuel remaining after achieving low earth orbit limits the payload mass that can be taken forward to the depot for refueling. If a similar DRM is ever contemplated for a cargo vehicle to Mars, propellants to refuel the vehicle would have to be prepositioned in Low Earth Orbit (like the payload) to maximize the payload mass.

For the propellant tank configurations used, and the fuel transfer pipe dimensions chosen (10 meters by 0.1 meters), canister fuel tanks appear to offer a competitive alternative to bulk fuel transfers. Although the use of canisters results in increased boiloff compared to the use of larger bulk fuel tanks, the bulk fuel tanks incur chilldown losses which negate their advantages when large numbers of shipments are involved.

The use of canisters often limits the use of the full payload capacity of the host vehicle. This was seen most vividly when shipping water in canisters on the LTV to a depot in GEO. Each LTV could only carry a single canister of water, leaving almost a third of its payload capacity unused, and greatly increasing the number of LTV flights required.

Optimization of the DRM vehicles for their assigned tasks is both possible and necessary. The sensitivity analyses revealed the LTV with 2 engines performed better than the LTV with one engine. More detailed trade studies are needed to determine the right balance between MLI mass and predicted losses to boiloff. Studies looking at canister tanks should also consider the increased mass of connecting hardware over that for bulk tanks.

## Acknowledgments

The authors thank Mr. Patrick S. McRight, Manager of the Propulsion Systems Design & Integration Division at Marshall Space Flight Center, who contributed his expertise regarding the complexities of cryogenic propellant storage and transfer.

The authors thank Mr. Steven G. Sutherlin, a Propulsion Systems Engineer in the Marshall Space Flight Center Advanced Concepts Office, who contributed his expertise regarding spacecraft design and its influence on propellant boiloff, and the characterization of the thermal environment.

The authors thank Mr. Larry Kos, a mission designer in the Marshall Space Flight Center Advanced Concepts Office, who contributed his expertise regarding the thrust-to-weight ratio for lunar vehicles.

The authors thank Mr. Robert Werka, a Senior Aerospace Flight Systems Engineer at Marshall Space Flight Center, contributed his expertise regarding rocket engine oxidizer-to-fuel ratios.

The authors thank Dr. Alan Wilhite, Distinguished Langley Professor of Advanced Aerospace Systems Architecture at the Georgia Institute of Technology, who contributed his expertise regarding the Modified Lockheed Model.

This paper was adapted from thesis work completed for the University of North Dakota in November, 2015. Individuals seeking additional information should contact the primary author at [thomas.m.perrin@nasa.gov](mailto:thomas.m.perrin@nasa.gov).

## References

- <sup>1</sup>London, J. R. (1994). *LEO on the Cheap*. Maxwell Air Force Base, AL: Air University Press.
- <sup>2</sup>Watson, K., Murray, B., and Brown, H. (1961) The Behavior of Volatiles on the Lunar Surface. *J. Geophys Res.*, 66, 3033-3045.
- <sup>3</sup>Arnold, J. R. (1979). Ice in the Lunar Polar Regions. *Journal of Geophysical Research*, 84(10), 5659-5668. doi:10.1029/JB084iB10p05659
- <sup>4</sup>Spudis, P. (2011) The Moon: Port of Entry to Cislunar Space. In C.D. Lutes and P.L. Hays (Eds.) *Toward a Theory of Spacepower*. (pp.241-251). Washington, DC: National Defense University Press.
- <sup>5</sup>Spudis, P. D., & Lavoie, A. R. (2011, September). *Using the resources of the Moon to create a permanent, cislunar space faring system*. Paper presented at AIAA SPACE 2011 Conference & Exposition, Long Beach, CA.
- <sup>6</sup>Huzel, D. K., & Huang, D. H. (1992). *Modern Engineering for Design of Liquid Propellant Rocket Engines*. Washington, DC: AIAA.
- <sup>7</sup>Chato, D. (2005). *Low gravity issues of deep space refueling* (NASA/TM—2005-213640). Retrieved from National Aeronautics and Space Administration website: <http://ntrs.nasa.gov/archive/nasa/casi.ntrs.nasa.gov/20050196665.pdf>
- <sup>8</sup>Oeffering, R. C. (2011). *A Cis-Lunar Propellant Infrastructure for Flexible Path Exploration and Space Commerce* (NASA/TM-2012-217235). NASA/Glenn Research Center.
- <sup>9</sup>Aerojet Rocketdyne. (2015). RL10 Engine. Retrieved from <http://www.rocket.com/rl10-engine>
- <sup>10</sup>NASA. (2005). *NASA's Exploration Systems Architecture Study (Final Report)* (NASA/TM-2005-214062). U.S. Government Printing Office.
- <sup>11</sup>Cook, S. (2008, September). *Lunar Program Industry Briefing; Ares V Overview*. Retrieved from [http://www.nasa.gov/pdf/278840main\\_7603\\_Cook-AresV\\_Lunar\\_Ind\\_Day\\_Charts\\_9-25%20Final%20rev2.pdf](http://www.nasa.gov/pdf/278840main_7603_Cook-AresV_Lunar_Ind_Day_Charts_9-25%20Final%20rev2.pdf)
- <sup>12</sup>Kyle, E. (2010, February 1). Space Launch Report: New Launchers - Ares V. Retrieved from [www.space-launchreport.com/ares5.html](http://www.space-launchreport.com/ares5.html)
- <sup>13</sup>Sostaric, R. R., & Merriam, R. S. (2008, February). *Lunar ascent and rendezvous trajectory design*. Paper presented at American Astronautical Society/31st Annual
- <sup>14</sup>George, L. E., & Kos, L. D. (1998). *Interplanetary Mission Design Handbook: Earth-to-Mars Mission Opportunities and Mars-to-Earth Return Opportunities 2009–2024* (NASA/TM—1998–208533). Marshall Space Flight Center, AL: National Aeronautics and Space Administration.
- <sup>15</sup>Thornton, E. A. (1996). *Thermal Structures for Aerospace Applications*. Reston, VA: American Institute of Aeronautics & Astronautics.
- <sup>16</sup>Planets and Pluto: Physical Characteristics. (2008, November 5). Retrieved from [http://ssd.jpl.nasa.gov/?planet\\_phys\\_par](http://ssd.jpl.nasa.gov/?planet_phys_par)
- <sup>17</sup>Wertz, J. R., & Larson, W. J. (Eds.). (2010). *Space Mission Analysis and Design* (3rd ed.). New York, NY: Microcosm Press & Springer.
- <sup>18</sup>Sheldahl Materials Corporation. (2015). *The Red Book [product specification handbook]*. Northfield, MN: Sheldahl Materials Corporation.
- <sup>19</sup>Hastings, L. J., Hedayat, A., & Brown, T. M. (2004). *Analytical Modeling and Test Correlation of Variable Density Multilayer Insulation for Cryogenic Storage* (NASA/TM-2004-213175). NASA/Marshall Space Flight Center.
- <sup>20</sup>Chai, P., & Wilhite, A. (2013). *Cryogenic Thermal System Analysis for Orbital Propellant Depot*. Acta Astronautica.